Three-dimensional photon confinement in photonic crystals of low-dimensional periodicity

P.R.Villeneuve
S.Fan
S.G.Johnson
J.D.Joannopoulos

Indexing terms: Photon confinement, Photonic crystals, Low-dimensional periodicity, Radiation loss

Abstract: Photonic crystals of one- or two-dimensional periodicity can be used to achieve three-dimensional photon confinement in dielectric waveguides with modal volumes of the order of a cubic half-wavelength. Since photonic crystals of low-dimensional periodicity do not have full three-dimensional bandgaps, the microcavities undergo increasing radiation losses with decreasing modal volumes. High-Q resonant modes can be generated by reducing the strength of the photon confinement. Increasingly, larger modal volumes lead to lower radiation losses and more efficient coupling to waveguide modes outside the cavity.

1 Introduction

The confinement of light to small volumes has important consequences on the properties of optical emission. The density of electromagnetic states, for example, can be significantly modified, and spontaneous emission can be either enhanced or inhibited. Confined systems can lead to the reduction in size and power requirement of integrated optical components, to single-mode operation of light-emitting devices, to the reduction of lasing thresholds in semiconductor lasers, and to higher modulation speeds [1].

Photonic bandgap (PBG) materials, also known as photonic crystals, offer a method of achieving strong photon confinement within volumes on the order of $(\lambda/2n)^3$, where λ is the emission wavelength and n is the refractive index [2, 3]. The localised states arise from the introduction of local defects inside photonic crystals. The large index contrast which exists between the different materials, necessary for achieving full three-dimensional bandgaps, causes the amplitude of the electromagnetic fields to fall off sharply away from the defect, resulting in strong photon confinement.

Three-dimensional crystals have the ability to completely isolate a mode from its surroundings by opening a gap along every direction in space. The fabrication of three-dimensional crystals, however, poses a great technological challenge. Several different geometries have been suggested for the fabrication of three-dimensional photonic crystals [4–10], but crystals with lower-dimensional periodicity may provide a more viable alternative for achieving strong photon confinement in dielectric structures.

One important aspect of structures with lower-dimensional periodicity is the coupling to radiation modes. By reducing the dimensionality of the crystal, and by resorting to standard index guiding to confine light along the nonperiodic directions, one no longer has the ability to contain light completely, and leaves open possible decay pathways through which light can escape.

In this paper, we investigate three-dimensional confinement of light in low-dimensional photonic crystals. We show that strong three-dimensional confinement can be provided in part by a photonic crystal, and in part by index confinement. We present a complete modal analysis, and investigate the coupling of confined optical modes to nonguided radiation modes.

2 Slab-waveguide microcavities

We consider a dielectric slab waveguide with a two-dimensional photonic crystal. The photonic crystal is used to confine light in the plane of the waveguide (say the xy-plane). It is up to the dielectric slab itself to keep light from escaping along the transverse direction (the z-direction). The modes inside the structure are highly dependent on the finite nature of the waveguide along the z-axis. The dimensions of the waveguide constitute an integral part of the problem.

We begin by investigating a uniform slab waveguide, and consider the effect of adding a periodic array of holes. This approach is preferable over the reverse approach, which consists of starting from a purely two-dimensional photonic crystal and 'adding' the finite nature of the structure along the z-direction, since purely two-dimensional structures lack information along the third dimension, making impossible the transition from an infinite structure to a finite structure.

We choose a slab waveguide with a large refractive index (n = 3.4) and, for simplicity, assume that the waveguide lies in air [11, 12]. (The effects of setting the waveguide on a substrate will be discussed below.) The thickness of the slab is 0.5 a where a is a scaling parameter which we define later. The use of a high-index waveguide is twofold; first, the high index provides strong field confinement along the z-direction (i.e.

IEE Proceedings online no. 19982467

Paper first received 3rd June 1998 and in revised form 28th October 1998

The authors are with the Department of Physics, Massachusetts Institute of Technology, Cambridge, MA 02139, USA

the extent of the guided modes outside the waveguide is small) allowing a large fraction of each mode to interact with the photonic crystal. Second, a high-index contrast is required between the dielectric material and the holes to open a bandgap in the xy-plane.

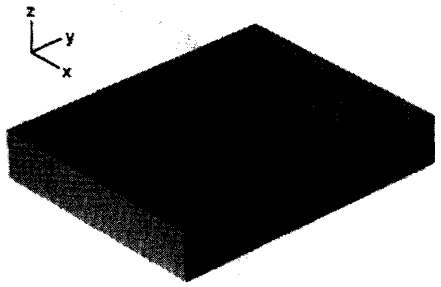

Fig. 1 *Schematic diagram of dielectric slab waveguide of thickness 0.5 a and refractive index 3.4*

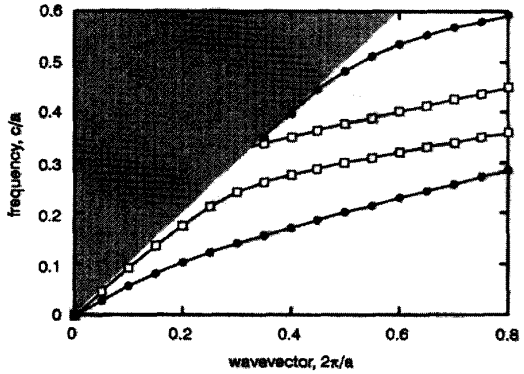

Fig. 2 *Band diagram of slab waveguide shown in Fig. 1*
● even, □ odd
Solid lines correspond to guided modes; shaded region corresponds to continuum of radiation modes; guided modes are labelled even or odd with respect to xy-plane of symmetry in middle of slab

The slab is shown in Fig. 1. Its corresponding dispersion relation is shown in Fig. 2. The solid lines correspond to guided modes; the shaded region corresponds to the continuum of radiation (i.e. nonguided) modes. The guided modes are labelled even and odd with respect to the horizontal plane of symmetry in the xy-direction, in the middle of the waveguide. We have chosen this labelling convention over the more traditional TE and TM convention since TE and TM modes are not strictly defined in slabs of finite extent (finite in the x or y directions) such as strip waveguides. Odd modes, for example, are characterised by the absence of electric field components in the x and y directions at the centre of the waveguide. A quantum well located at the centre of the waveguide could be designed such that light from the well would be unable to couple to the odd modes. The dispersion relation is plotted using the scalable parameter a which is defined below.

The band structure shown in Fig. 2 is continuous; there is no upper bound on the wavevector. The introduction of a periodic array of holes into the slab waveguide has the effect of limiting the wavevector, folding the dispersion relation into the first Brillouin zone, and splitting the guided-mode bands. Fig. 3 shows a slab waveguide with a triangular array of holes. The holes have a radius of 0.30 a, where a is the lattice constant of the array. The associated band structure is shown in Fig. 4. Again, the shaded region above the light line corresponds to the continuum of radiation modes. Below the light line, modes remain perfectly guided and propagate undisturbed through the holes without loss. A gap can be seen between the first and second even bands.

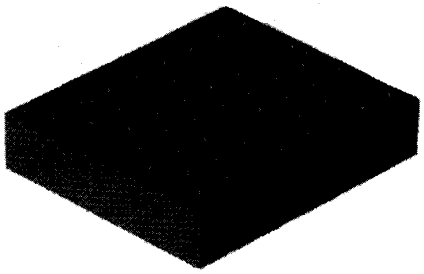

Fig. 3 *Schematic diagram of slab waveguide with two-dimensional array of holes with radius 0.3 a, where a is lattice constant of periodic array*
Parameters of slab are identical to those in Fig. 1

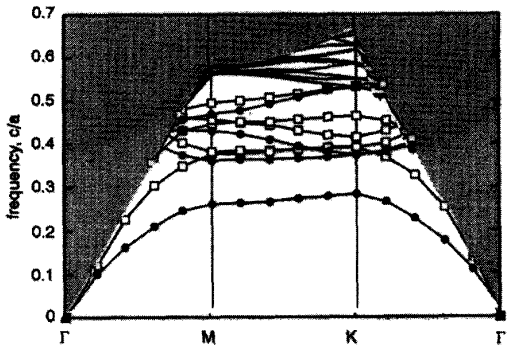

Fig. 4 *Band diagram for slab waveguide shown in Fig. 3*
Only lowest nine bands are labelled even and odd, to avoid overloading Figure; guided modes do not exist above cut-off frequency of 0.66 c/a

The introduction of holes in the waveguide has two other effects; first, it creates a frequency cut-off for guided modes. Every mode above the frequency 0.66 c/a is folded into the radiation continuum, and is Bragg scattered out of the slab. The cut-off frequency is independent of the refractive index of the slab or the size of the holes, and depends only on the lattice geometry of the array of holes. The other effect consists of shifting the guided modes to higher frequencies. The shift arises from the removal of high-index material in the holes, resulting in a reduction of the effective index of the waveguide. The shift has implications for mode matching between the mode in the PBG section and the one in the uniform (i.e holeless) section, and for radiation loss from the PBG slab.

For purposes of comparison, we show in Figs. 5 and 6 the corresponding structure and band diagram for a purely two-dimensional system. The structure can be viewed as a slab of infinite thickness with no field variation along the z-axis. The dielectric material is chosen to have the same index of refraction as the waveguide above, with holes of equal size. Fig. 6 shows how strongly the band diagram is affected by the finite nature of the structure along the z-axis.

If a defect is introduced in the PBG structure shown in Fig. 3, localised states can be formed in the vicinity of the defect. Since each localised state has a specific symmetry with respect to the mirror plane, it is possible to create an even state between the first and second even bands, orthogonal to odd states.

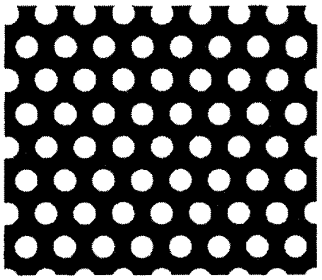

Fig. 5 *Schematic diagram of purely two-dimensional photonic crystal*
Dielectric material has refractive index of 3.4 and holes have radius of 0.3 *a*

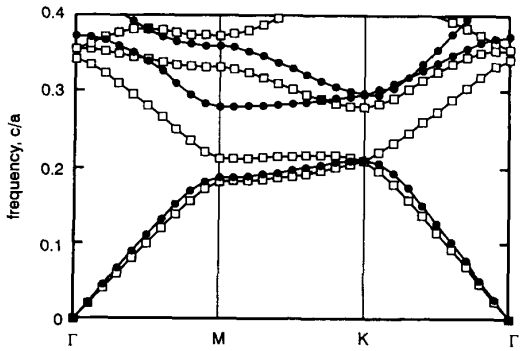

Fig. 6 *Band diagram of two-dimensional crystal shown in Fig. 5*

If, for example, light were to originate from a quantum well located at the middle of the waveguide, atomic transitions could be made to couple only to even modes. Figs. 7*a* and *b* show the electric-field energy density of such a localised state for the case where a single hole has been removed from the periodic array. The resonant state is doubly degenerate, and has a dipole-like symmetry in the horizontal plane. Its frequency is centred at 0.30 *c*/*a*.

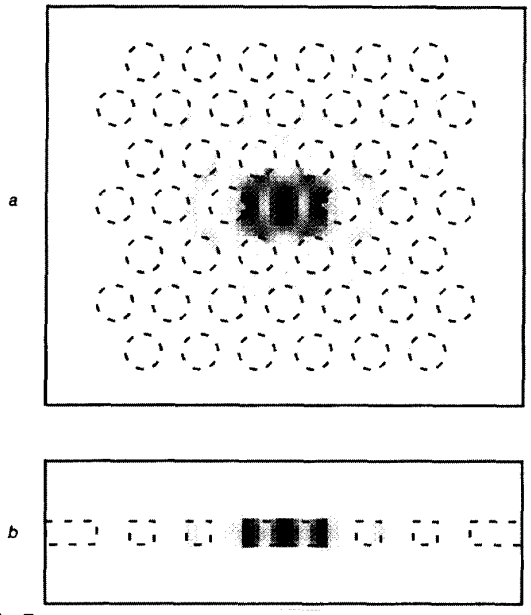

Fig. 7 *Electric-field energy density of three-dimensionally confined state inside slab waveguide with two-dimensional array of holes*
Energy density is shown in two different planes:
a Horizontal plane in middle of waveguide
b Vertical *yz*-plane
Peaks in energy density are shown in black; zero energy density is shown in white; dashed lines indicate edges of dielectric material; localised state is created by filling single hole; quality factor Q_{tot} of state is 240

Two competing decay mechanisms contribute to the overall decay rate of this resonant state; coupling to guided modes in the waveguide (the desired decay mechanism) and decay to radiation modes. Because the resonant mode is strongly localised in real space, it is highly extended in wavevector space. Limiting the coupling between this mode and the radiation continuum is necessary to achieve efficient coupling to guided modes. The total quality factor of the resonant mode Q_{tot} is a measure of the optical energy stored in the microcavity over the total cycle-average power radiated out of the cavity. It is defined as $f/\Delta f$, where Δf is the width of the resonance, and it is given by [13]:

$$\frac{1}{Q_{tot}} = \frac{1}{Q_{wg}} + \frac{1}{Q_{rad}} \tag{1}$$

where $1/Q_{wg}$ is a measure of the coupling to waveguide modes and $1/Q_{rad}$ is a measure of the coupling to radiation modes. To compute Q_{tot}, we use a finite-difference time-domain computational scheme [14] which first involves pumping energy into the cavity, and monitoring its decay. A resonator can sustain a total of Q_{tot} oscillations before its energy decays by a factor $e^{-2\pi}$ (or approximately 0.2%) of its original value. A more detailed description of this procedure can be found elsewhere [15]. The mode shown in Figs. 7*a* and *b* has a quality factor Q_{tot} of 240.

Since the structure does not have a complete three-dimensional bandgap, Q_{rad} is finite. Hence, it is not possible to increase mode confinement and Q_{tot} indefinitely. As the mode confinement increases, coupling to radiation modes also increases, and eventually dominates over coupling to guided modes inside the waveguide. Moreover, coupling to radiation modes are enhanced when the waveguide is positioned on top of a substrate. The substrate provides a favourable escape route, and may cause significant radiation loss. It will be shown, however, in the following Section that strong field confinement and low loss can be achieved when dielectric waveguides are located on low-index materials.

By itself, Q_{tot} is not sufficient to determine the fraction of the energy which is coupled to guided modes, and the fraction which is coupled to radiation modes. By increasing the modal volume of the localised state, we can reduce the coupling to radiation modes (i.e. increase Q_{rad}) and, provided the coupling to guided modes remains largely unchanged, increase Q_{tot}. The modal volume can be increased, for example, by creating a different type of defect in the structure. If, instead of removing a single hole from the two-dimensional array, we reduce the radius of seven nearest-neighbour holes from 0.3 *a* to 0.2 *a* otherwise leaving the structure unchanged, the dipole-like mode shown in Figs. 7*a* and *b* would become more extended in real space and its Q_{tot} would increase to 2500. (The new resonant state has the same frequency as the one shown in Figs. 7*a* and *b*).

3 Strip-waveguide microcavities

Instead of using a slab waveguide and a two-dimensional photonic crystal, we also could have used a strip waveguide (to confine light along two dimensions) and a one-dimensional photonic crystal (to confine light along the third dimension). The basic strip-waveguide

structure is shown in Fig. 8 with its corresponding dispersion relation in Fig. 9. The waveguide consists of a high-index strip (such as silicon; n = 3.48 at λ = 1.55μm) on a low-index layer (such as SiO_2; n = 1.44). The low-index layer separates the guided mode from the underlying high-index substrate, and allows for strong field confinement.

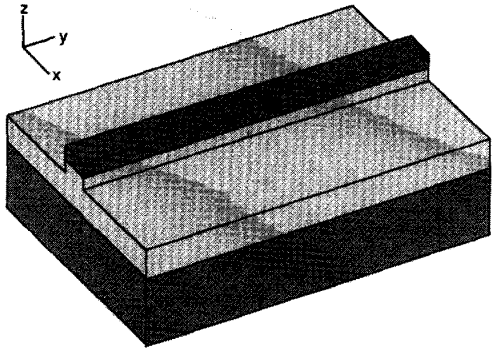

Fig. 8 *Schematic diagram of high-index strip waveguide (n = 3.48) on low-index layer (n = 1.44)*
Waveguide has dimensions 0.4 a × 1.2 *a* and is single mode over wide frequency range

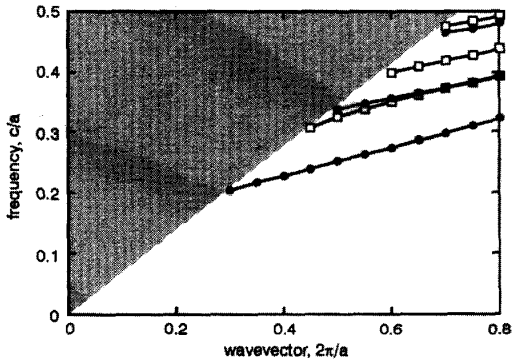

Fig. 9 *Band diagram of waveguide shown in Fig. 8*
● even, □ odd
Solid lines correspond to guided modes; shaded region corresponds to continuum of radiation modes; guided modes are labelled even or odd with respect to *xy*-plane in middle of high-index strip

The guided modes are shown by solid lines in Fig. 9. The modes are labelled even and odd with respect to the horizontal plane in the middle of the strip waveguide. We should point out that the horizontal plane is not a perfect plane of symmetry for this system. The presence of a low-index layer and a substrate breaks the symmetry along the z-axis. However, the mode classification based on the horizontal plane remains approximately valid when the refractive index of the underlying layer is low, and when the thickness of the layer is large enough to isolate the modes from the substrate. The horizontal plane provides a very useful classification scheme. Again, in the case where light originates from a quantum well located at the middle of the strip waveguide, atomic transitions could be made to couple only to even modes.

The shaded region in Fig. 9 corresponds to the continuum of radiation modes. The slope of the light line is determined by the refractive index of the low-index layer. This layer increases the coupling of the defect state (which we will introduce shortly) to the radiation modes. Fig. 10 shows a strip waveguide with an array of holes. The holes have the effect of folding the guided-mode bands into the first Brillouin zone. In addition to showing modes lying below the light line, Fig. 11 shows 'guided' bands which are folded inside the radiation continuum. These leaky-mode bands, which are shown by white bars, are not truly guided. Since modes above the light line are free to leak out of the guide, they behave like resonant states with a specific 'lifetime'. The lifetime inside the waveguide depends on the losses, which in turn depend on the coupling strength to the radiation modes, which, in turn, depends on the strength of the perturbation (i.e. the size of the holes). The bars are used to indicate that each data point has a certain frequency width, though no effort was made to correlate the length of the bars to the lifetime of the modes.

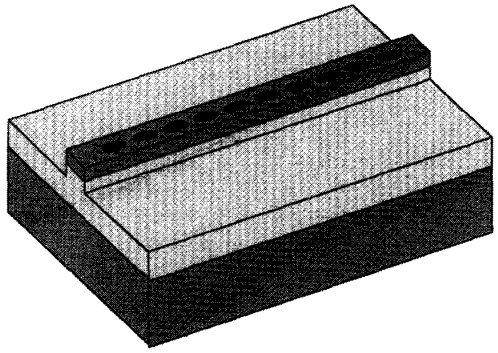

Fig. 10 *Schematic diagram of strip waveguide with one-dimensional array of holes of radius 0.23 a*
Parameters of waveguide are identical to those in Fig. 8

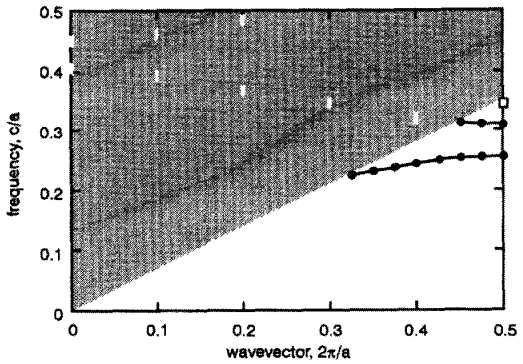

Fig. 11 *Band diagram for waveguide shown in Fig. 10*
Guided modes do not exist above cut-off frequency of 0.35 c/a; white bars correspond to leaky modes folded into radiation continuum

The solid black lines correspond to guided modes which exist in spite of the presence of holes. The modes do not leak out. When a defect is introduced in the periodic array, the defect mode, which is made up primarily of guided modes, couples far less to radiation modes than it would if, say, the defect state was located above the light line in the second-order gap.

Before showing a defect state, we show, in Figs. 12 and 13, the band diagram for a purely one-dimensional structure. The even and odd modes are degenerate. It is clear, upon inspection of Figs. 11 and 13 that the finite nature of the waveguide plays a significant role in shaping the band diagram of the one-dimensional photonic crystal.

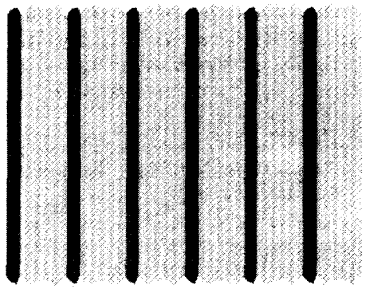

Fig. 12 *Schematic diagram of purely one-dimensional photonic crystal*
High-dielectric material has refractive index of 3.48 and low-dielectric material has refractive index of 1.00

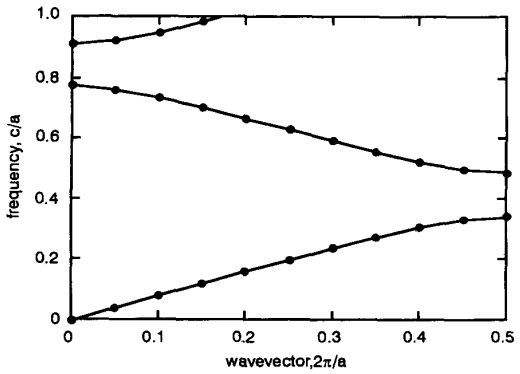

Fig. 13 *Band diagram of one-dimensional crystal shown in Fig. 12*

We now investigate the radiation losses of a defect state. We introduce a defect in the hole array, as shown in Fig. 14, and create a state inside the bandgap. The resonant mode is strongly confined within the microcavity and has a frequency of 0.27 *c/a*. The modal volume, *V*, is defined by [3]:

$$VP_{max} = \int P(\mathbf{r}) d^3\mathbf{r} \qquad (2)$$

where $P(\mathbf{r})$ is the total electromagnetic energy density of the mode and P_{max} is the peak value of $P(\mathbf{r})$. Using this definition, a modal volume of 0.004 a^3 is computed, where a is the lattice constant of the periodic hole array, which corresponds to a volume of only five times $(\lambda/2n)^3$.

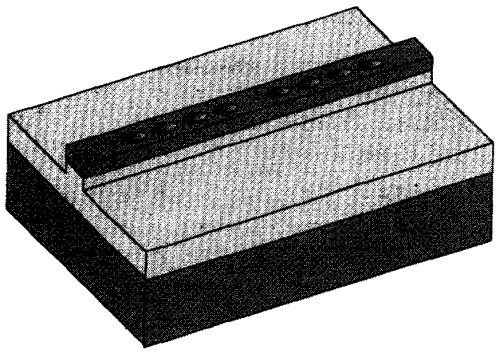

Fig. 14 *Schematic diagram of strip-waveguide microcavity*
Parameters of waveguide are identical to those shown in Fig. 10

Using again a finite-difference time-domain scheme, we compute the transmission through the structure [14]. Results are shown in Fig. 15. The computation shows a wide bandgap, and a sharp resonant peak with a quality factor Q_{tot} of 280. Transmission outside the gap is large which suggests that the modes remain guided as they propagate through the holes, and undergo little scattering. At resonance, the coupling efficiency exceeds 82%. The coupling occurs from the waveguide mode via the evanescent field through the array of holes. By increasing the number of holes, the reflectivity of the array is increased. However, as we increase the number of holes, we also increase the radiation losses, hence reduce the throughput of the microcavity. The peak transmission through the cavity is given by:

$$T_{max} = \frac{Q_{tot}^2}{Q_{wg}^2} \qquad (3)$$

For the structure shown in Fig. 14, we find a value for Q_{wg} of 310. As T_{max} approaches unity, Q_{wg} becomes equal to Q_{tot} and, from eqn. 1, Q_{rad} becomes infinitely large. In this case, the cavity mode would decay entirely into the waveguide.

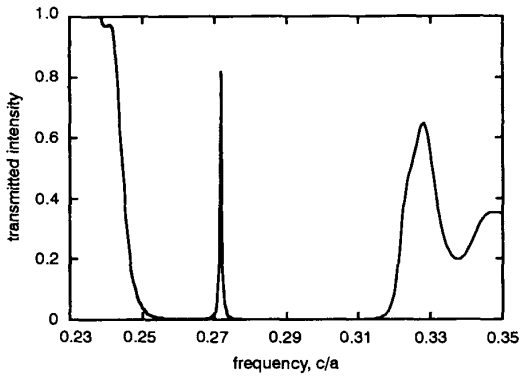

Fig. 15 *Transmission properties of waveguide microcavity shown in Fig. 14*
At resonance, transmission exceeds 82%; the three-dimensionally confined state has quality factor Q_{tot} of 280

Now, by coupling an optical transition to the microcavity resonance, the spontaneous emission rate can be enhanced by a factor η over the rate without a cavity. The expression for η is given as [16]:

$$\eta = \frac{Q_{tot}}{4\pi V}\left(\frac{c}{n\nu}\right)^3 \qquad (4)$$

where ν is the optical transition frequency. For the specific strip-waveguide microcavity described above, the maximum enhancement is calculated to be 35, which is significantly larger than any enhancement yet measured. This large spontaneous emission enhancement could lead to faster modulation of optical devices, and to the development of zero-threshold lasers.

4 Microcavities operating above the light line

The existence of bandgaps between leaky-mode bands above the light line (as shown in Fig. 11) suggests that it may also be possible to create defect states above the light line, though these defect states couple more heavily to radiation modes. A demonstration of this effect was published by Krauss *et al.* in 1997 [17]. They used an $Al_{.12}Ga_{.88}As$ waveguide (n = 3.5) on an $Al_{.35}Ga_{.65}As$ layer (n = 3.3). Instead of using holes, the authors elected to use deep and narrow grooves. A schematic diagram of the structure is shown in Fig. 16.

We compute the band diagram for this structure and show the results in Fig. 17, both with and without

grooves on the same plot. The slope of the light line is determined by the index of $Al_{.35}Ga_{.65}As$. The solid black region corresponds to guided modes. At a frequency of 0.50 *c/a*, for example, there are 18 modes tightly packed close to the light line. Since the mode density is large, we did not label the modes according to their symmetry, to avoid overloading the figure. Moreover, the horizontal plane does not constitute a valid plane for mode characterisation in this case since the waveguide is highly asymmetric in the vertical direction.

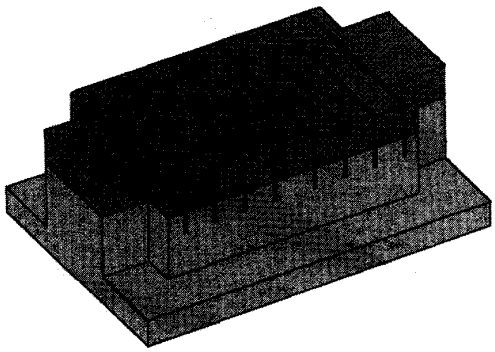

Fig. 16 *Schematic diagram of strip-waveguide microcavity designed to operate above light line*
Strip has thickness of 0.9 *a*, width of 9.0 *a* and refractive index of 3.5, and lies on layer of index 3.3; grooves are 1.6 *a* deep and 0.2 *a* long

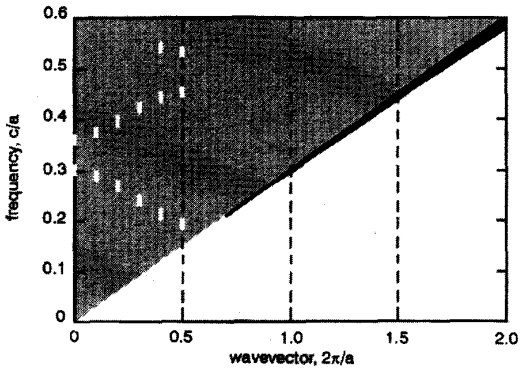

Fig. 17 *Band diagram of waveguide shown in Fig. 16 with and without grooves*
Black region corresponds to guided modes in absence of grooves; at frequency of 0.5 c/a, for example, there are 18 modes tightly packed close to light line; white bars correspond to leaky modes folded into radiation continuum in presence of grooves; leaky mode is shown only for lowest guided mode

When grooves are added to the uniform waveguide, every mode is folded into the radiation continuum. We show in Fig. 17 the folded lowest-order mode. The length of the white bars is not meant to correspond exactly to the frequency width of the mode. By introducing a defect, the authors created a state at frequency 0.49 *c/a* above the light line, in the third-order gap. Although Fig. 17 shows only one folded resonant band, several of them are present, each coupling to a different degree with the incoming mode. If the incoming mode is the lowest order waveguide mode, the largest coupling should occur with the lowest-order resonant mode.

We compute the transmission using again a finite-difference time-domain method. The simulations are carried out in two dimensions since the three-dimensional computational cell is too large. We assume that the structure is infinite in the lateral direction (i.e. we assume an infinitely wide waveguide, with no field variation along that direction). The two-dimensional simulations resemble the case of the lowest order mode. Results are shown in Fig. 18. The transmitted intensity through the array of grooves is normalised to the intensity in a uniform waveguide without grooves.

The edges of the third-order gap match well with those published in [17]. The large Fabry–Perot fringes outside the gap are due to the small number of grooves. At resonance, the transmission efficiency is close to 4%. The resonance is centered at 0.49 *c/a*, and it has a quality factor Q_{tot} close to 1000. The modal volume of the experimental structure exceeds the one presented in the previous Section by more than two orders of magnitude [Note 1]. While guided modes outside the gap propagate through the grating with an efficiency of up to 65%, the resonant mode experiences severe loss as it 'bounces' back and forth, roughly one thousand times, inside the cavity before escaping. As it spends more time inside the cavity, the resonant mode couples increasingly to radiation modes. From eqns. 1 and 3, we find $Q_{wg} = 5000$ and $Q_{rad} = 1250$. One could increase transmission at resonance by reducing Q_{wg} which would have the effect of reducing the total time light spends inside the cavity. However, if transmission is to be made comparable to the one presented in the previous Section, it will be paramount for Q_{rad} to remain much greater than Q_{wg}. Any reduction of the modal volume will result in a reduction of Q_{rad}. To achieve a large value for both Q_{rad} and T_{max} while maintaining a very small modal volume, the cavity must be operated in a gap below the light line.

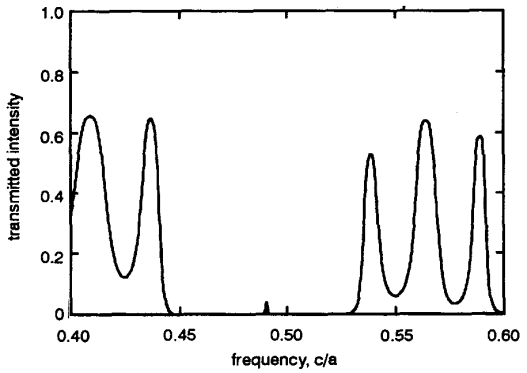

Fig. 18 *Transmission properties of waveguide microcavity shown in Fig. 16*
Transmission at resonance is 4%; quality factor Q_{tot} is close to 1000; transmission could be made larger than 4% by reducing Q_{wg}

5 Conclusion

We have presented a rigorous modal analysis of photon confinement in dielectric structures. We have shown that strong field confinement and low radiation loss can be achieved in microcavities using a combination of the PBG effect and index confinement. These microcavities readily lend themselves to microfabrication, and do not require elaborate three-dimensional lithography processing. Furthermore, by including quantum wells inside the waveguides, these microcavities may provide a means to fabricate ultra-fast and ultra-low-threshold optical devices.

Note 1: The lateral dimension of the resonant mode was assumed to be equal to the width of the waveguide. This approximation should yield an underestimate of the mode volume.

6 Acknowledgment

This work was supported in part by the MRSEC Program of the NSF under Award DMR-9400334.

7 References

1 YOKOYAMA, H., and UJIHARA, K. (Eds.): 'Spontaneous emission and laser oscillation in microcavities' (CRC Press, Boca, Raton, 1995)
2 YABLONOVITCH, E., GMITTER, T.J., MEADE, R.D., RAPPE, A.M., BROMMER, K.D., and JOANNOPOULOS, J.D.: 'Donor and acceptor modes in photonic band structure', *Phys. Rev. Lett.*, 1991, **67**, (24), pp. 3380–3383
3 FORESI, J.S., VILLENEUVE, P.R., FERRERA, J., THOEN, E.R., STEINMEYER, G., FAN, S., JOANNOPOULOS, J.D., KIMERLING, L.C., SMITH, H.I., and IPPEN, E.P.: 'Photonic-bandgap microcavities in optical waveguides', *Nature*, 1997, **390**, pp. 143–145
4 YABLONOVITCH, E., GMITTER, T.J., and LEUNG, K.M.: 'Photonic band structure: the face-centered-cubic case employing nonspherical atoms', *Phys. Rev. Lett.*, 1991, **67**, (17), pp. 2295–2298
5 HO, K.M., CHAN, C.T., SOUKOULIS, C.M., BISWAS, R., and SIGALAS, M.: 'Photonic band gaps in three dimensions: new layer-by-layer periodic structures', *Solid State Commun.*, 1994, **89**, pp. 413–416
6 SÖZÜER, H.S., and DOWLING, J.P.: 'Photonic band calculations for woodpile structures', *J. Mod. Opt.*, 1994, **41**, pp. 231–239
7 FAN, S., VILLENEUVE, P.R., MEADE, R.D., and JOANNOPOULOS, J.D.: 'Design of three-dimensional photonic crystals at submicron lengthscales', *Appl. Phys. Lett.*, 1994, **65**, (11), pp. 1466–1468
8 CHENG, C.C., and SCHERER, A.: 'Fabrication of photonic band-gap crystals', *J. Vac. Sci. Technol. B*, 1995, **13**, (6), pp. 2696–2700
9 ROMANOV, S.G., JOHNSON, N.P., FOKIN, A.V., BUTKO, V.Y., YATES, H.M., PEMBLE, M.E., and SOTOMAYOR TORRES, C.M.: 'Enhancement of the photonic gap of opal-based three-dimensional gratings', *Appl. Phys. Lett.*, 1997, **70**, (16), pp. 2091–2093
10 FEIERTAG, G., EHRFELD, W., FREIMUTH, H., KOLLE, H., LEHR, H., SCHMIDT, M., SIGALAS, M.M., SOUKOULIS, C.M., KIRIAKIDIS, G., PEDERSEN, T., KUHL, J., and KOENIG, W.: 'Fabrication of photonic crystals by deep X-ray lithography', *Appl. Phys. Lett.*, 1997, **71**, (11), pp. 1441–1443
11 VILLENEUVE, P.R., FAN, S., JOANNOPOULOS, J.D., LIM, K.Y., PETRICH, G.S., KOLODZIEJSKI, L.A., and REIF, R.: 'Air-bridge microcavities', *Appl. Phys. Lett.*, 1995, **67**, (2), pp. 167–169
12 KANSKAR, M., PADDON, P., PACRADOUNI, V., MORIN, R., BUSCH, A., YOUNG, J.F., JOHNSON, S.R., MACKENZIE, J., and TIEDJE, T.: 'Observation of leaky slab modes in an air-bridged semiconductor waveguide with a two-dimensional photonic lattice', *Appl. Phys. Lett.*, 1997, **70**, (11), pp. 1438–1440
13 HAUS, H.A.: 'Waves and fields in optoelectronics' (Prentice–Hall, Englewood Cliffs, 1984), chap. 7
14 KUNZ, K.S., and LUEBBERS, R.J.: 'The finite-difference time-domain method for electronics' (CRC Press, Boca, Raton, 1993)
15 FAN, S., WINN, J.N., DEVENYI, A., CHEN, J.C., MEADE, R.D., and JOANNOPOULOS, J.D.: 'Guided and defect modes in periodic dielectric waveguides', *J. Opt. Soc. Am. B*, 1995, **12**, (7), pp. 1267–1272
16 YOKOYAMA, H., and BRORSON, S.D.: 'Rate equation analysis of microcavity lasers', *J. Appl. Phys.*, 1989, **66**, pp. 4801–4805
17 KRAUSS, T.F., VÖGELE, B., STANLEY, C.R., and DE LA RUE, R.M.: 'Waveguide microcavity based on photonic microstructure', *IEEE Photonics. Technol. Lett.*, 1997, **9**, (2), pp. 176–178